Vol. A53 (1978) ACTA PHYSICA POLONICA No 2

THE REFERENCE COORDINATE APPROACH FOR DETERMINING THE MINIMUM ENERGY REACTION PATH*,**

By R. F. Nalewajski*** and T. S. Carlton****

Department of Chemistry, University of North Carolina, Chapel Hill

(Received July 30, 1977)

The reference coordinate approach is presented for locating transition states and the minimum energy reaction paths (MERP's) on potential energy surfaces (PES's). It treats the PES, $E(x, y, L)$, as $E_r[x, y, L(x, y)]$; x and y are the mapping coordinates, and L stands for the remaining coordinates. A reference curve (RC) is used to generate a good approximations to the MERP, as the locus of minima in sections perpendicular to the RC. Two kinds of RC are used: the bond-energy-bond-order (BEBO) path and an energy contour (EC) that passes from reactants to products. General algorithms are proposed for following EC's and for recognizing that an EC has entered a product region. Results obtained with the BEBO paths as RC for the H_2+H and H_2+F systems are reported. The efficiency of the method is illustrated by application to model "blind" valley surfaces, using an EC as RC.

1. Introduction

The *transition-state* (activated-complex) *theory* [1] of chemical kinetics has provided for a wide variety of chemical reactions the most useful phenomenological framework for both parametrizing and calculating rate constants from the properties of the elementary species participating in the reaction and those of the activated complex. According to this theory a starting step in an a priori determination of a rate constant is a calculation of the *potential barrier*, and this is still valid even when the assumption of the existence of a long-lived activated complex is not justified [2]. The potential barrier is calculated along the *reaction profile*, a section through the *minimum-energy reaction path* (MERP), corresponding to the *saddle points* (S) and the bottoms of the *reactants* and *products valleys*

* Dedicated to Professor Kazimierz Gumiński on the occasion of his 70-th birthday.

** Aided by research grant to the University of North Carolina from the National Institutes of Health.

*** Permanent address: Department of Theoretical Chemistry, Institute of Chemistry, Jagellonian University, Krupnicza 41, 30-060 Kraków, Poland.

**** Permanent address: Department of Chemistry, Oberlin College, Oberlin, Ohio 44 074, U. S.A.

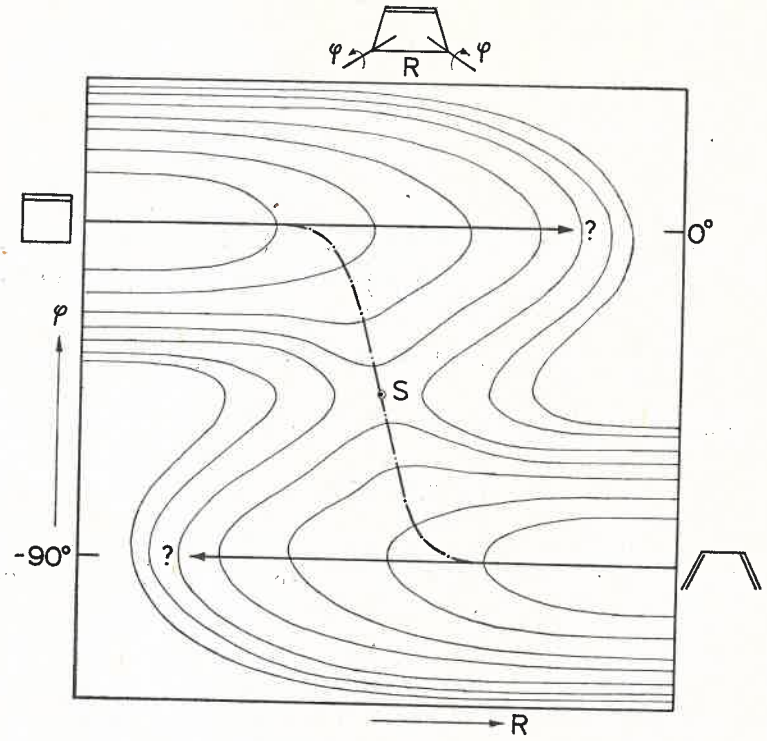

a

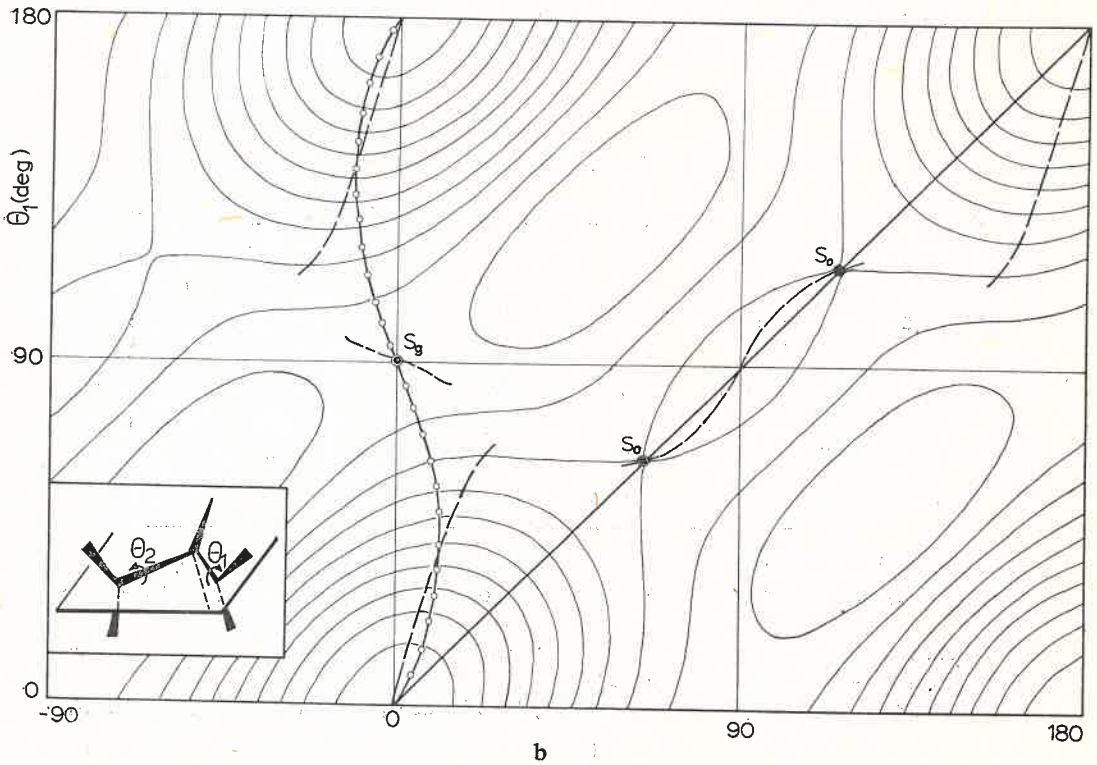

b

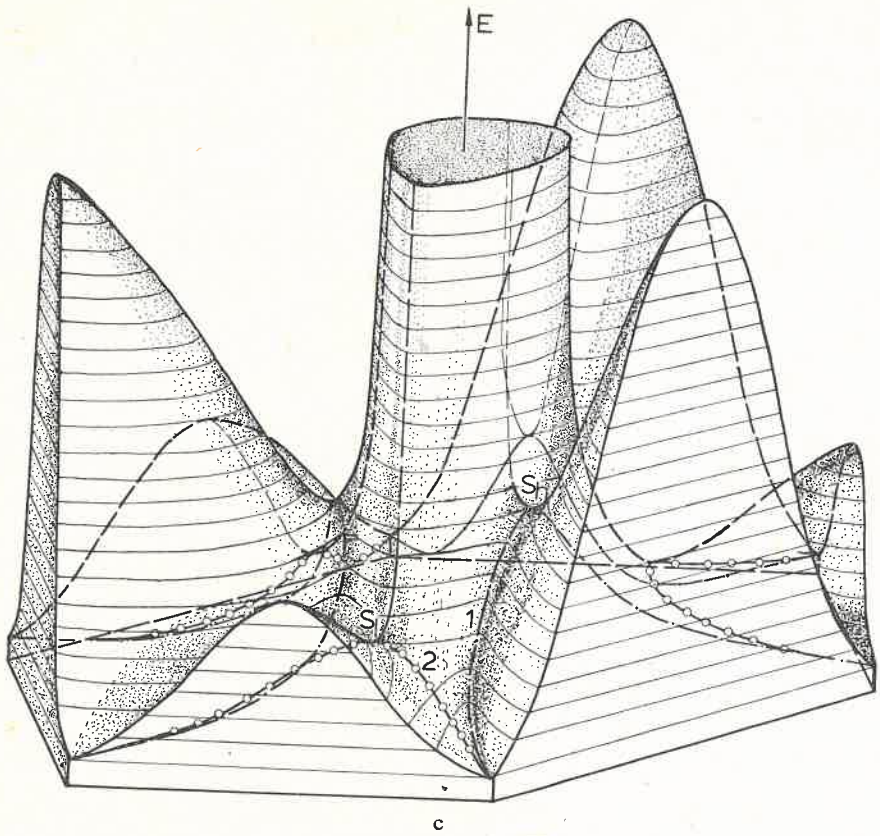

Fig. 1. Examples of the potential energy surfaces showing inadequancy of the "following the bottom" and "reaction coordinate" algorithms: (a) Schematic energy contour diagram of the two "blind" valleys surface for the rearrangement of cyclobutene into butadiene by disrotatory ring opening (Refs [18, 31]). Both the "following the bottom" and "reaction coordinate" techniques (the latter using R as independent variable) are inadequate to find the pass between the reactant and product valleys. (b) Contour diagram of the potential energy surface used to model isomerizations of the trimethylene diradical (Ref. [36]). The "following the bottom" algorithm will give only the optical isomerization path (solid line), being inadequate to find higher pass along the geometrical isomerization path (circles). The discontinuous path (broken line) has been obtained by applying the mapping coordinate θ_1 as "reaction coordinate". The energies (in kcal/mol) are relative to the zero energy configuration ($\theta_1 = 0$, $\theta_2 = 0$), and the gap between two successive contours is 0.5 kcal/mol. (c) Perspective view of the potential-energy surface for H_3, based on the data reported in Ref. [37]. The "following the bottom" procedure will reach the higher saddle point S_h along the path (1) (— · —), missing the lower pass through the saddle point S_1 lying on the path (2) (circles)

(see Fig. 1). The concept of a reaction path as used here is a static property of the given potential energy surface, and is distinct from that of a classical trajectory.

The main sources of potential energy surfaces are calculations based on the methods using empirical energy functions [3], Extended Hückel Theory (EHT [4]), various versions of the ZDO SCF MO schemes (CNDO [5], INDO [6], MINDO [7], and NDDO [8]), the Perturbative-Configuration-Interaction-of-Localized-Orbitals method (PCILO [9]), and ab initio schemes [10]. Most of the systematic dynamical studies, however, utilize not

ab initio surfaces but rather model surfaces generated by various versions o the London-Eyring-Polanyi (LEP) method [11], the Diatomic-in-Molecules (DIM) method [12], and many arbitrary function models, e.g. [13].

In recent years much effort has been devoted to the development of reliable methods for exploring potential energy surfaces, i.e. locating both the stationary and saddle points, and determining the MERP [14–24]. The search techniques applied may be classified according to whether or not they make the assumption of choosing one degree of freedom as the independent variable of the potential energy (called "*reaction coordinate*" [18]), and optimizing the remaining degrees of freedom for each value of the independent variable. The "*reaction coordinate*" *algorithms* have proved to be inadequate in many cases(e.g. [18, 22, 25]), often giving discontinuous paths (Fig. 1), and sometimes failing to include the transition state. The second, *general approach* involves consideration of all the degrees of freedom, and can in turn be decomposed into whether or not the algorithms seek to locate only chemically interesting points on the complete hypersurface [17, 20, 24], rather than to follow the MERP along the bottom of the reactant and product valleys [14, 19, 23]. The former methods, perhaps the most promising, involve the use of symmetry [15] and generation of the "linear" and "quadratic" internal paths to locate initially the transition state region, with subsequent minimization of the norm of the gradient. The latter, although providing quite satisfactory following of bottom of the valley, will obviously fail in the case of a pass between the reactant and product valleys that is located on the side of ridge as shown in Fig. 1a. It will also be inadequate to find a second pass from a given valley, higher (Fig. 1b) or lower (Fig. 1c), being designed only to follow closely the bottom of the valley.

The purpose of this article is to describe a simple method for quickly locating the transition state region and MERP. The method uses the *reference coordinate*, defined here quite generally as any smooth curve leading from reactants to products through transition state region, and displaying the main features of the surface in question. This definition is similar to those used by Marcus [26a] and Light [26b]. The method proposed is to some extent conceptually similar to those involving generation of arbitrary paths [17, 20, 24]. Also, it allows one to avoid the abovementioned disadvantages of the "bottom-following" procedure. The illustrative applications of the method to the collinear exchange reaction surfaces (the $H+H_2$ and H_2+F systems) and model "blind" valley surfaces are reported. As the reference coordinates the BEBO trajectory [27] and a contour of the surface in the "mapping" plane were used respectively.

2. *The reference coordinate approach*

The potential energy functions are in general multidimensional. The most common manner of their graphical representation (for a description of the surface topographically) is by contour maps. Such a map is constructed by representing two variables (*mapping coordinates*) as distances along the x and y axes. The potential energy function is then considered as an explicit function of only x and y, with all the other variables (*relaxational coordinates*) either held fixed or optimized for each point on the mapping plane (see

Appendix A). The former case is really a two-dimensional cut through a multidimensional surface. The latter, on the other hand, represents the reduced picture of the complete surface on the (x, y) plane, including the effect of changes in molecular skeleton via relaxational degrees of freedom, which is valid in most cases.

The choice of x and y is not generally unambiguous. Nevertheless, one can make good choices in most cases, by taking into account the expected changes in geometry. As a general rule one uses coordinates that are common to both reactants and products, and that undergo considerable change in the course of reaction. For instance, in disrotatory ring opening of cyclobutene (Fig. 1a) the axes $x = \varphi$ and $y = R$ can be chosen.

The "raction coordinate" method (using one of the mapping coordinates as the independent variable) often fails to produce smooth, continuous paths [25]. This is because the one-dimensional cuts through a surface which it uses to determine the "MERP" are not perpendicular in general to the exact MERP. Herein lies the basic difficulty, since such perpendiculars cannot be determined a priori in the general case. We introduce the *reference curve* (RC) in the mapping plane as a means to generate good approximations to these exact perpendiculars. This will be possible if the RC is smooth and *well behaved*, i.e., *leading from reactants to products through the transition state region, and displaying the main features of the surface.* The locus of the energy minima along the perpendiculars to the RC define the *reference coordinate path* (RCP). The RCP is expected to lie rather close to the MERP when the RC is well behaved. This approach, to be called the *reference coordinate approach*, can also be applied iteratively by using the RCP obtained in a previous iteration as the RC for determining the next RCP, until self-consistency is reached.

For instance, in the case of collinear exchange reactions the BEBO trajectory [27] or Light's curve [26b] can be applied as the starting RC. The illustrative applications of the BEBO RC will be the subject of the next section.

The BEBO RC is obviously not of general applicability. Alternatively, we here wish to suggest the use of the *energy contours* (EC) on a mapping plane for quickly exploring a general surface, i.e. for finding the pass from reactants to products and for determining the corresponding RCP. In order to follow efficiently a contour of the potential energy surface we have developed a contour-following algorithm (described in Appendix A) with rather substantial reduction in computational effort within ZDO SCF MO type calculations.

A contour can be used as the RC for generating an RCP only if the contour crosses a transition-state region. Therefore, in addition to generating a contour, one must decide whether it enters a region associated with reaction products. Techniques for making this decision are described briefly in Appendix B. Starting in the reactant region with a contour whose energy is expected to be lower than that of the saddle point one determines contours of successively higher energy until one is found to enter the product region. This approach is also applicable to cases in which there are several sets of products. For each set of products one then generates an RCP as though that set were the only one.

The treatment described here provides the MERP and the corresponding saddle-points S_Q on the reduced potential energy surface $E[\boldsymbol{Q}, \boldsymbol{L}(\boldsymbol{Q})]$, which depends explicitly only on the mapping coordinates $\boldsymbol{Q}$; $\boldsymbol{L}$ denotes the remaining, relaxational degrees of

freedom of molecular system. To locate the exact saddle-point S on the multidi-mensional surface $E(\boldsymbol{Q}, \boldsymbol{L})$ further calculations are necessary to refine the point S_Q. As shown by McIver and Komornicki [17, 24], such refinement can be efficiently accomplished by the minimization of the gradient norm, $|\boldsymbol{g}(\boldsymbol{Q}, \boldsymbol{L})|$, using the least-squares method of Powell [38]. The extra computational work should be small, because one can expect S_Q to be close to S.

3. Application of the BEBO reference curve to the collinear exchange reactions

Johnston and Parr [27a] have used the idea of the conservation of the overall bond order n during the "bond-breaking-bond-forming" process leading to exchange reaction. They assume that

$$n_1 + n_2 = 1, \tag{1}$$

where n_1 and n_2 are the bond orders of the two bonds in question. Equation (1) when combined with the Pauling relation [28],

$$R_i = R_i^{(s)} - a_i \log(n_i), \quad n_i \in [0,1], \tag{2}$$

defines the *bond-energy-bond-order* (BEBO) *trajectory*. $R_i^{(s)}$ is the length of the "standard" bond i (with $n_i = 1$) and a_i is an empirical constant. The BEBO trajectory has been reported to represent quite satisfactorily the MERP of exchange reactions (e.g., [27b, c]. This suggests that it can be used profitably as the reference curve, BEBO RC, for determining a more refined path, BEBO RCP.

We have chosen two collinear exchange reactions as illustrative examples:

(*i*) $H + H_2 \rightarrow H_2 + H$, with the SCF CI surface of Shavitt and coworkers [29],

(*ii*) $F + H_2 \rightarrow FH + H$, with the LEPS surface of Muckermann [30].

These reactions, having a symmetrical and asymmetrical two-valley surfaces, respectively, were reported previously as typical examples of the inadequacy of a single "reaction coordinate" procedure for determining the course of the reaction [25]. The results, obtained using the BEBO parameters from Ref. [27c], are summarized in Figs 2, 3.

Figure 2 shows that the "reaction coordinate" technique generates a "kink" in the reaction path near the saddle-point when R_{12} is used as reaction coordinate to the right of the saddle point and R_{23} is used to the left [25a]. The BEBO RCP, on the other hand, represents a "kinkless" path, slightly refined in comparison with the BEBO path, and, as follows from inspection of the contour map, practically identical with the MERP. Similar conclusions follow from Fig. 3. One can observe, however, that deviations of the discontinuous "reaction coordinate" paths from the MERP (Fig. 3a) are much larger in the case of $H_2 + F$ than those for H_3. As a result the corresponding profiles (Fig. 3b) lead through the region of much higher energy near both ends, where the largest deviations can be observed. Again one can see that the BEBO RC generates the BEBO RCP, which is practically the exact MERP.

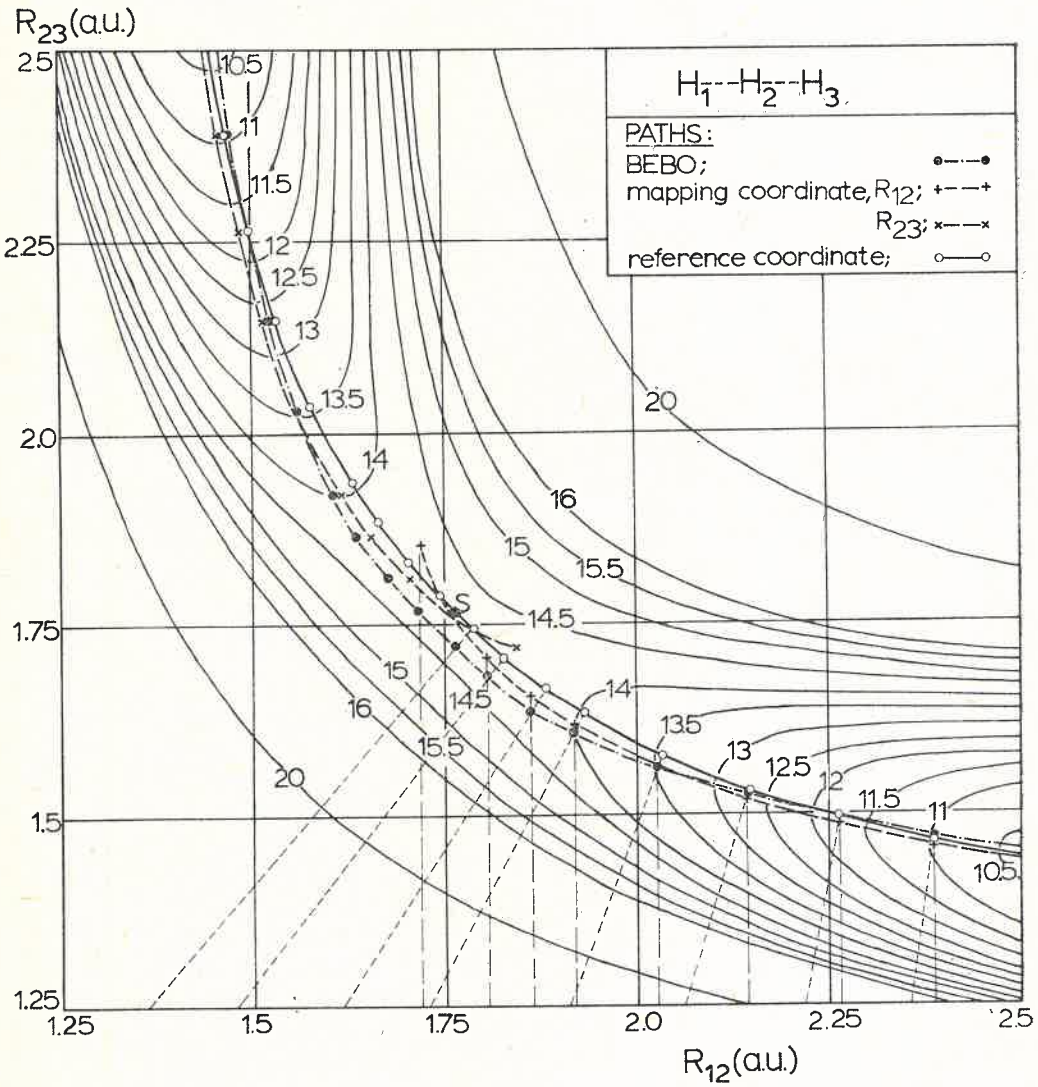

Fig. 2. Application of the BEBO trajectory for determination of the MERP on the surface for collinear exchange reaction of the $H+H_2$ system. The potential surface were taken from Ref. [29]. The discontinuous paths obtained by searching for the minimum in the directions perpendicular to both mapping coordinates are also shown. The parameters of the BEBO curve were taken from Ref. [27c]

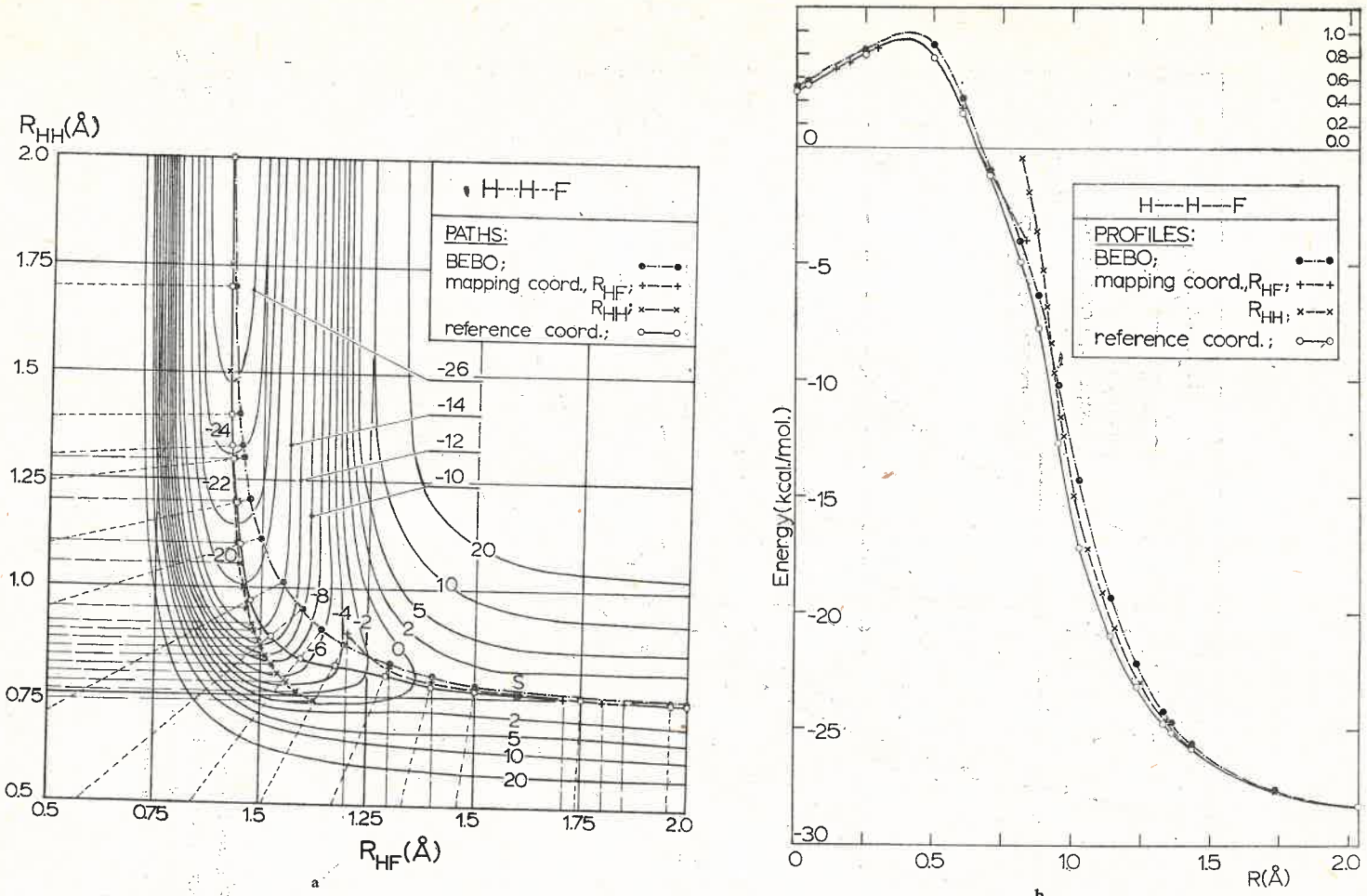

Fig. 3. Application of the BEBO trajectory for determination of the MERP on the surface for collinear exchange reaction of the H_2+F system: (a) paths, (b) energy profiles. The Muckerman LEPS potential energy surface [30] has been used. The discontinuous paths obtained by searching for the minimum along the directions perpendicular to both mapping coordinates are also shown (a) together with corresponding profiles (b). The parameters of BEBO curve were taken from Ref. [27c]

4. Use of the energy contours in exploring the model "blind" valley surfaces

Dewar et al. [18, 31] have observed that a single geometric coordinate is inadequate for following the course of pericyclic reactions that involve antiaromatic transition states. Potential W_3 (Eq. (3)) models the singnificant features of the surfaces for these reactions, namely two "blind" valleys that are connected by a pass through the ridge that separates them (Fig. 1a).

$$W_3 = W_{\text{ridge}} - W_{\text{pass}} + W_{\text{end}}, \tag{3}$$

$$W_{\text{ridge}} = [E_{\text{ridge}}/(1-2A)^2]\,\{1+2A^2+A[A\exp(-2x/x_v)-2\exp(-x/x_v) + A\exp(2x/x_v)-2\exp(x/x_v)]\}, \tag{3a}$$

$$A = \exp(-x_v)/[1+\exp(-2x_v)], \tag{3b}$$

$$W_{\text{pass}} = \tfrac{1}{2}(E_{\text{ridge}}-E_{\text{pass}})\,[1+\cos(\pi x/x_v)]\exp(-y^2/B^2), \tag{3c}$$

$$W_{\text{end}} = \tfrac{1}{4}C[1-\cos(\pi x/x_v)]\,\{1+\tanh[([-x/|x|]y-D)/F]\}. \tag{3d}$$

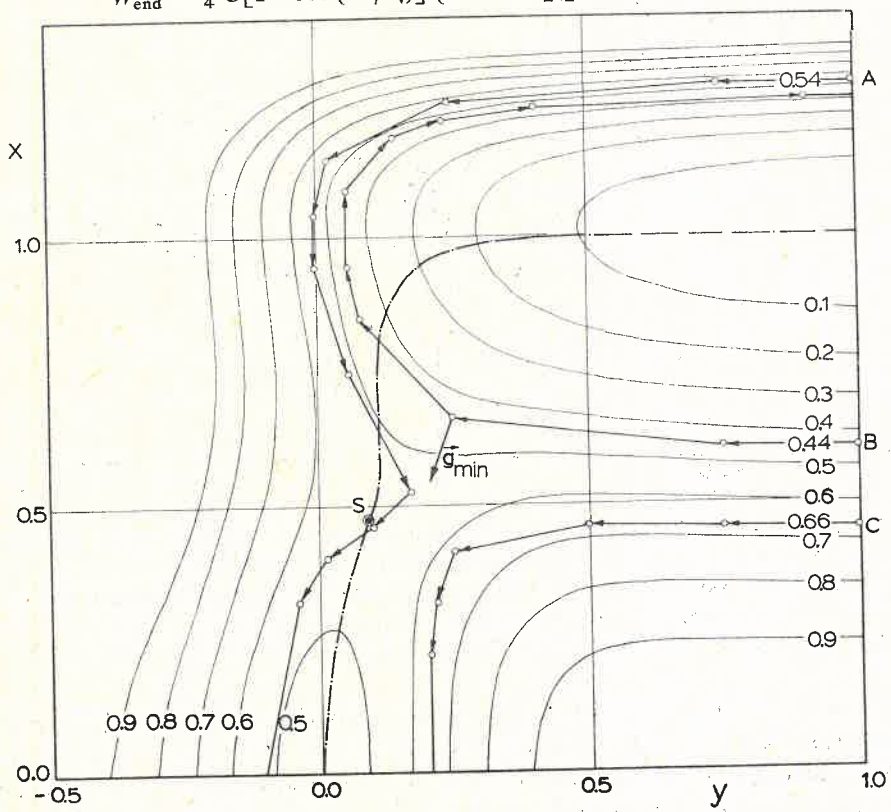

Fig. 4. Use of the equipotential contours as the reference coordinates in searching for the transition state region and the MERP on the model "blind" valley surface I, having a basin at the pass between the reactant and product valleys. The origin of the coordinate system is the center of symmetry for the equipotential contours. The saddle point S occurs early before the middle of the pass. The values of the surface parameters (see text) are: $E_{\text{ridge}} = 1.0$, $x_v = 1.0$, $E_{\text{pass}} = 0.45$, $B = 0.3$, $F = 0.5$, $C = 2.0$, and $D = 0.25$. The contours, A, B, and C refer to $\gamma = 0.5$ (see Appendix A).

The origin of the coordinate system is at the centre of the pass, which is the center of symmetry for the equipotential contours. The ridge lies on the y-axis, and the two valleys are parallel to it. W_{ridge} (Eqs (1a) and (1b)) is a cross-section perpendicular to the ridge at a value of y that is well removed from the pass or either valley end. W_{ridge} is the

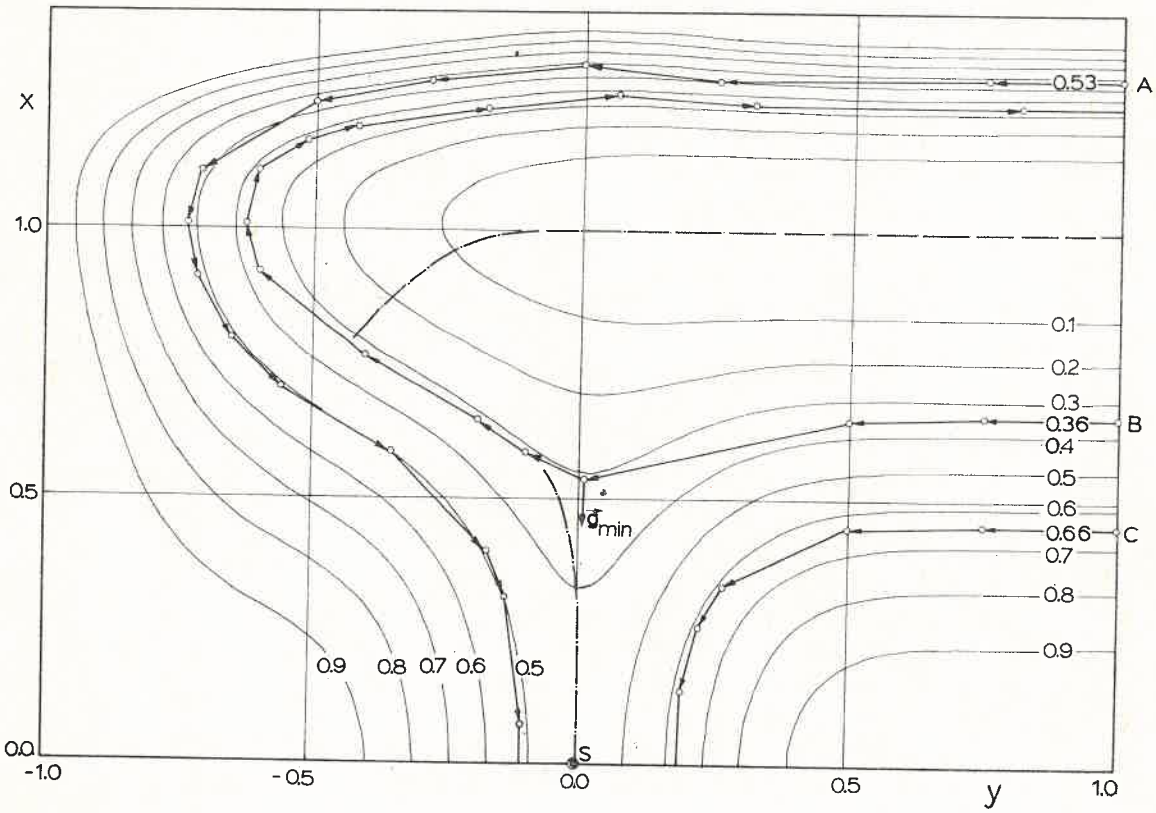

Fig. 5. Use of the equipotential contours as the reference coordinates in searching for the transition state region and the MERP on the model "blind" valley surface II, having a saddle point S at the middle of the pass. The origin of the coordinate system is the center of symmetry for the equipotential contours. The values of the surface parameters (see text) are: $E_{\text{ridge}} = 1.0$, $x_v = 1.0$, $E_{\text{pass}} = 0.45$, $B = 0.3$, $F = 0.5$, $C = 2.0$, and $D = 1.0$. The contours A, B, and C refer to $\gamma = 0.5$ (see Appendix A)

symmetric version of the back-to-back Morse functions used by Löwdin [32], W_{ridge} is re-expressed, however, to make the valley floors the zero of the energy, E_{ridge} the height of the ridge, and x_v the distance from the ridge to the minimum of either valley. W_{pass} introduces the pass through the ridge without affecting the valley floors. W_{end} closes the valley ends without affecting E_{pass}, the energy at the midpoint of the pass. If the valley ends are sufficiently far from the pass, E_{pass} is the activation energy for the reaction (Fig. 5). If the valley ends interact strongly with the pass, a basin can be formed at the pass (Fig. 4). In this event there is s transition state on each side of the ridge, and the activation energy is greater than E_{pass}.

We have used the potential W_3 (Eq. (3)) to test the validity of the reference coordinate approach based on the use of energy contours as reference curves. Two "blind" valley surfaces have been generated: I (Fig. 4), including a basin in the middle of the pass between "reactant" and "product" valleys, and II (Fig. 5), with the saddle at the middle of the pass and the ends of the valleys more "pathologically" distant from the pass. Note that similarly to the situation shown in Fig. 1a, both the "bottom-following" technique and the use of y as a "reaction coordinate" miss completely the pass to the next valley.

The contour-following procedure has been applied to investigations of there representative contours (A, B, and C) on both surfaces. Among these contours A and C have higher energy than the sadle-point, whereas B has a lower energy. The RCP's shown in both figures have been obtained using contour C as the RC. The assumed tolerance of the energy deviation in the contour-following algorithm (see Appendix A) was $t = 0.05$.

Both figures show that the contour-following procedure constitutes a quite efficient way for determining the pass to the next valley. Figure 4 shows that the RCP is a continuous path leading from the "reactant" valley through a saddle-point S and the bottom of the basin to the "product" region. Visual inspection of the contour map shows, however, that the RCP is slightly different from the expected MERP. This is because the RC used (contour C) is not a good enough approximation to the MERP. Note, however, that using the RCP shown in Fig. 4 as the RC should give a much better RCP in the next iteration. Figure 5 shows that the "blind" valley feature of surface II is so "pathological" that use of contour C as a reference curve does not generate a continuous path. In such a case perhaps the only way to obtain the MERP is first to locate the saddle-point and then, starting from this point, to move in small steps in accordance with the steepest-descent direction towards the "reactant" and then towards the "product" valleys. One can observe, finally, that the minimum gradients on the "nonreactive" contours B have been located quite satisfactorily in spite of large step sizes applied (maximum step size = 0.5), showing in both cases the direction of the pass to the next valley. On the basis of these test results one can expect that the finite step size applied in the contour-following procedure (controlled in our algorithm by the current curvature of the contour) should not introduce a significant error when the second test of Appendix B is used for recognizing that an energy contour has entered a product region.

The authors are deeply grateful for the hospitality accorded them in Professor Robert G. Parr's group at the University of North Carolina at Chapel Hill. The authors are also much indebted to Dr. Robert A. Donnelly for providing a copy of the program SCANB for plotting the contour diagrams, and for his assistance in using this program.

APPENDIX A

The algorithm for following of constant-energy contours

It is desirable to base the algorithm for the contour following on a local quadratic approximation to the surface $E[\boldsymbol{Q}, \boldsymbol{L}(\boldsymbol{Q})]$, where $\boldsymbol{Q} = (x, y)$ denotes the two mapping coordinates and $\boldsymbol{L} = (L_3, \ldots, L_f)$ is the set of the remaining internal degrees of freedom

of a molecular system. The parameters $\boldsymbol{L}$ are assumed to be either fixed or partly optimized for a given point $\boldsymbol{Q}$. Within the SCF MO methods the total energy depends on nuclear coordinates also through the matrix of the SCF LCAO MO coefficients, $\boldsymbol{C}[\boldsymbol{Q}, \boldsymbol{L}(\boldsymbol{Q})]$. It was shown recently [33], however, that in the case of the ZDO type od SCF MO calculations practically complete optimization of structural parameters can be performed using the fixed matrix $\boldsymbol{C}(\boldsymbol{R}_0)$, where $\boldsymbol{R}_0$ represents the starting point for optimization of geometry. Thus, within the widely used ZDO approximation (CNDO, INDO(MINDO), and NDDO methods) such partial refining of the parameters $\boldsymbol{L}(\boldsymbol{Q})$ for a given point $\boldsymbol{Q}_k$ can be rather efficiently carried out with negligible additional computational expense by using the fixed matrix $\boldsymbol{C}(\boldsymbol{Q}_k, \boldsymbol{L}_k))$. The first-order contribution to the energy expansion near point $[\boldsymbol{Q}_k, \boldsymbol{L}(\boldsymbol{Q}_k)]$ is expected to be negligible; $\boldsymbol{L}(\boldsymbol{Q}_k))$ collects the relaxational structural parameters determined from the condition of the vanishing forces

$$F_i(\boldsymbol{Q}_k, \boldsymbol{L}) \approx F_i^{(k)}[\boldsymbol{Q}_k, \boldsymbol{L}; \boldsymbol{C}(\boldsymbol{Q}_k, \boldsymbol{L}_k)] = 0, \quad i = 3, \ldots, f. \tag{A1}$$

The second-order contributions can be estimated [33a] using the force constants determined from the force field $\boldsymbol{F}^{(k)}$ [Eq. (A1)], e.g. via the finite difference method [17a, 34]. Also, to a good approximation parameters $\boldsymbol{L}$ can be held fixed at $\boldsymbol{L}(\boldsymbol{Q}_k)$ during the searching for the next point in the contour-following procedure. In what follows we will consider explicitly only mapping plane $\boldsymbol{Q} = (x, y)$ and the energy surface $E[\boldsymbol{Q}, \boldsymbol{C}(\boldsymbol{Q}_0)]$.

The quadratic approximation should ensure fast ultimate convergence for most surfaces when steps become small. Let us now assume that the following second-order

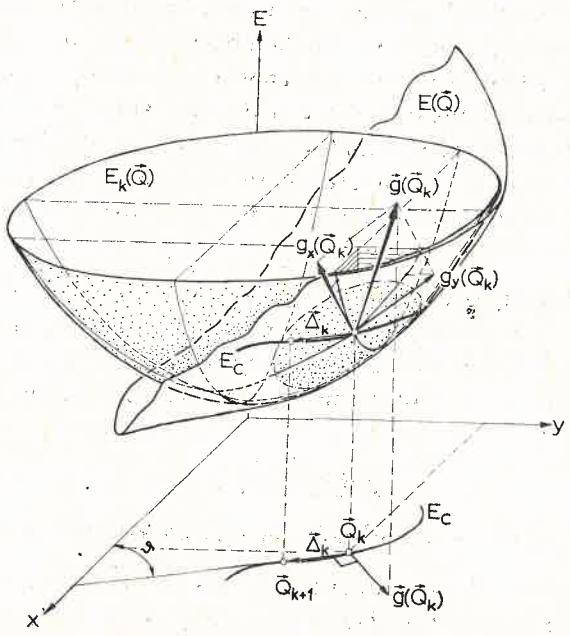

Fig. A1. Schematic picture illustrating the procedure used to follow the contour E_c on the surface $E(\boldsymbol{Q})$

Taylor expansion remains valid in the neighborhood of the point $Q_k = (x_k, y_k)$ (see Fig. A1):

$$E_k(Q) = E(Q_k) + g(Q_k)q^T + qH^{(k)}q^T, \tag{A2}$$

where for the current point Q_k

$$q = Q - Q_k, \tag{A2a}$$

$$g(Q_k) = \left[\left(\frac{\partial E}{\partial x}\right)_{Q_k} \left(\frac{\partial E}{\partial y}\right)_{Q_k}\right], \tag{A2b}$$

$$(H^{(k)})_{ij} = \tfrac{1}{2}\left(\frac{\partial^2 E}{\partial q_i \partial q_j}\right)_{Q_k}. \tag{A2c}$$

Energy gradients are provided directly by the ZDO-type methods [17a], and the Hessian matrix $H^{(k)}$ can be reasonably estimated from the force field $F^{(k)}$ $[Q, C(Q_k)]$ [33a], e.g. by finite differences [17a, 34],

$$H_j^{(k)} = \left(\frac{\partial g}{\partial q_j}\right)_{Q_k} \approx \frac{1}{4\delta}[g(q_+^{(i)}) - g(q_-^{(j)})], \tag{A3}$$

where δ is a small scalar and $q_\pm^{(j)}$ denotes the point with $q_j = \pm\delta$ and $q_{i\neq j} = 0$. In ab initio calculations both gradients and Hessian matrix require the finite difference approach [35], and the procedure described here becomes rather expensive.

In order to follow the contour E_c without excessive deviation from the starting energy we should look for vector $\alpha\Delta_k$ such that

$$\Delta E_k \equiv E(Q_k + \alpha\Delta_k) - E(Q_k) = -[E(Q_k) - E_c] \equiv -D_k, \tag{A4}$$

where α is set equal to unity at each step unless the calculated absolute value of the energy deviation D_{k+1} is greater than an assumed tolerance t, in which case α is halved and the step repeated. Approximating ΔE_k by the energy change estimated using Eq. (A2), we have

$$\Delta E_k \approx \alpha g(Q_k)\Delta_k^T + \alpha^2 \Delta_k H^{(k)} \Delta_k^T = -D_k. \tag{A5}$$

To obtain efficient yet close following of a contour the step size Δ_k should respond to changes in the contour curvature, c_k. Thus we use

$$\Delta_k = \gamma / c_k, \tag{A6}$$

where γ is a parameter that controls step size. Depending on the value of the ratio $s_k = g_1(Q_k)/g_2(Q_k)$, the curvature c_k is estimated from the relations:

$$c_k = \begin{cases} (s_k - s_{k-1})/\Delta_{1,k-1}, & \text{if } s \leqslant 1, \\ -\left(\dfrac{1}{s_k} - \dfrac{1}{s_{k-1}}\right)\Big/\Delta_{2,k-1}, & \text{if } s > 1. \end{cases} \tag{A7}$$

Finally, for a given step size Δ_k the equation (A5) is solved for the step direction ϑ (Fig. A1).

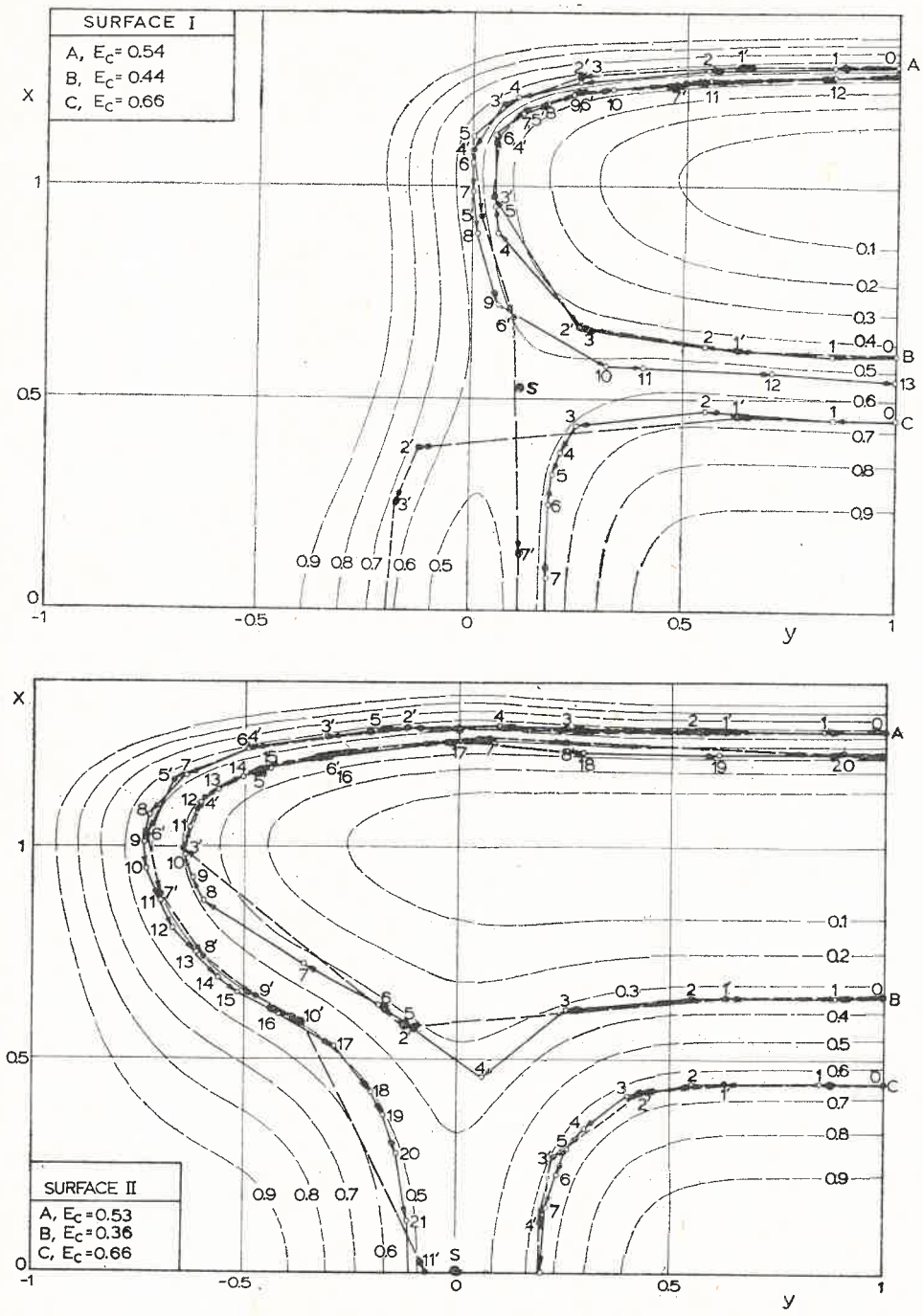

Fig. A2. Effect of the step size parameter, γ, on the contour-following on the "blind" valley surfaces I(a) and II(b). For the values of the surface parameters see Figs 4 and 5 respectively. The broken line (primed numbers) and solid line (nonprimed numbers) refer to the calculations with $\gamma = 0.75$ and $\gamma = 0.3$ respectively

A set of calculations for model "blind" valley surfaces, as described in a preceding section, have been carried out to test efficiency of the contour-following procedure. The maximum step size $\Delta_{max} = \gamma$ and the tolerance of the energy deviation $t = 0.05$ were assumed. Two values of γ, 0.3 and 0.75, have been used. The results are compared in Fig. A2.

The test calculations show that the following of the contour is very satisfactory, even for quite large step sizes ($\gamma = 0.75$). Notice that for such high values of the parameter γ only a very few steps are required for the complete testing of all the contours considered (the number of steps is the number of the function recalculation in the ZDO SCF MO approximation). It follows that the local quadratic approximation to the surface remains valid even for large steps. This tendency demonstrates the efficiency of the proposed algorithm. Reference to Fig. A2 also shows that the step size control we have adapted allows one to reproduce rather satisfactorily the shape of a contour. However Fig. A2a shows that for large step sizes and closely placed contours of the same potential energy, it is eventually possible to escape from one branch of the given contour into another. This fortunately does not affect the efficiency of the contour-following procedure in searching quickly for the pass between the reactant and product valleys, and in providing information about the shape of the minimum energy reaction path.

APPENDIX B

Techniques for recognizing that an energy contour has entered a product region

The first test requires that one knows in advance the approximate equilibrium location of the reaction products in which one is interested. At each step along a contour one tests whether a circle of given radius around this product location is intersected by the linear extension of the negative end of the gradient vector. The test works because the tail of the gradient vector must sweep over the product location at least once while the

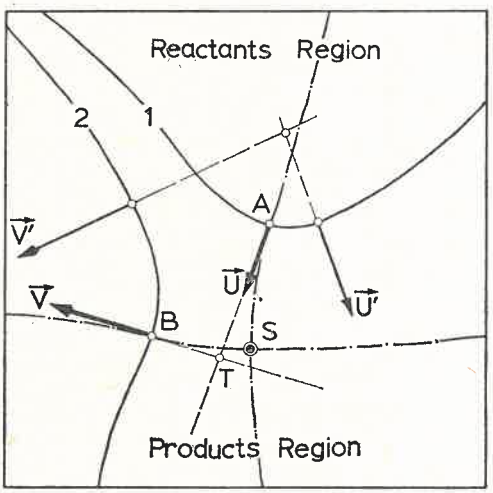

Fig. B1. Energy contours in the neighborhood of a saddle-points, *S*. Arrows are gradient vectors

contour is in the product region. The circle should be large enough to keep the vector's tail from jumping completely across the circle, between two consecutive steps of the contour--following algorithm. If one accepts a possitive outcome of the test only when the point on the contour is closer to the products than to the reactants (or to other sets of products, if any), the possibility of misleading results is small, though not zero. Such pathological cases will be detected when one attempts to construct an RCP using the contour as RC. The test is economical, since one already has the gradient at each point on the contour (see Appendix A). A little simple algebra is the only extra computation that is required.

The secondt est does not require any prior knowledge about location of reaction products. This test is based on properties of potential energy surfaces near any saddle-point, as illustrated by Fig. B1. In that figure curve AS is the MERP and curve BS is the crest of the region that separates reactants from products. The energy of contour 1 is less than that of the saddle-point whereas that of contour 2 is greater. Because point A lies on the MERP, the magnitude of its gradient $\vec{U}$ is a local minimum for its contour, and the vector points to the convex side of the contour. Because point B lies on a ridge, the magnitude of its gradient $\vec{V}$ is likewise a local minimum, but the vector points to the concave side. Vectors $\vec{U}$ and $\vec{V}$ are tangent to the MERP and the crest, respectively. Therefore the extension of the positive end of vector $\vec{U}$ intersects the extension of the negative end of vector $\vec{V}$ if their contours are sufficiently close in energy. The point of intersection, T, is then an approximation to the location of the sadle-point.

The details of the second test follow. Let $\vec{V}$ be a gradient vector that is a local minimim for the contour currently under study. Let $\vec{U}$ be the closest gradient vector that is a local minimum for the adjacent contour that is lower in energy. The outcome of the test is judged positive only if the positive extension of $\vec{U}$ intersects the negative extension of $\vec{V}$, if $\vec{U}$ points to the convex side of its contour, and if $\vec{V}$ points to the concave side of its contour. In this case one may assume that the contour of $\vec{V}$ crosses over into a product region, but the contour of $\vec{U}$ does not. Misleading results of this test can arise because of finite energy intervals or because of finite step lengths along the contours. Finite step length is the more serious. It can cause displacement of both vectors along their contours by distances up to the current step lengths. Displacement arises because a gradient vector is regarded as a local minimum merely if it is shorter than vectors at the steps immediately before and after its own. Figure B1 illustrates the resulting error when the vectors $\vec{U}'$ and $\vec{V}'$ are displaced from the true local minima $\vec{U}$ and $\vec{V}$, respectively.

In summary, the first test is more economical than the second, but it requires prior knowledge about the location of reaction products. The second test is more general because it does not require this knowledge, bur it requires smaller step sizes and energy intervals to attain reliability comparable with that of the first test.

REFERENCES

[1] The classic textbook reference to traditional transition-state theory is (a) S. Gladstone, K. J. Laidler, H. Eyring, *Theory of Rate Processes*, McGraw-Hill, New York 1941; for a brief historical discussion and bibliography see (b) K. J. Laidler, *Theories of Chemical Reaction Rates*, McGraw--Hill, New York 1969, pp. 41–55.

[2] S. G. Christov, *Berichte der Bunsen-Gesellschaft für Physikalische Chemie* **76**, 507 (1972).

[3] For example, see: (a) J. E. Williams, P. J. Stand, P. v. R. Schleyer, *Ann. Rev. Phys. Chem.* **19**, 531 (1969); (b) S. Lifson, A. Warshel, *J. Chem. Phys.* **49**, 5116 (1968); A. Warshel, S. Lifson, *J. Chem. Phys.* **53**, 8582 (1970); (c) R. A. Scott, H. A. Scheraga, *J. Chem. Phys.* **45**, 2091 (1966); H. A. Scheraga, *Adv. Phys. Org. Chem.* **6**, 103 (1968); L. I. Shipmann, A. W. Burgess, H. A. Scheraga, *Proc. Nat. Acad. Sci.* (USA) **72**, 543 (1975); (d) A. Warshel, M. Karlus, *J. Am. Chem. Soc.* **94**, 5612 (1973); B. R. Gelin, M. Karlus, *J. Am. Chem. Soc.* **97**, 6996 (1975).

[4] R. Hoffmann, *J. Chem. Phys.* **39**, 1397 (1963).

[5] J. A. Pople, G. A. Segal, *J. Chem. Phys.* **43**, S136 (1965).

[6] J. A. Pople, D. L. Beveridge, D. A. Dobosh, *J. Chem. Phys.* **47**, 2076 (1967).

[7] (a) N. C. Baird, M. J. S. Dewar, *J. Chem. Phys.* **50**, 1262 (1969); (b) M. J. S. Dewar, E. Haselbach, *J. Am. Chem. Soc.* **92**, 590 (1970); (c) R. C. Bingham, M. J. S. Dewar, D. H. Lo, *J. Am. Chem. Soc.* **97**, 1285 (1974).

[8] J. A. Pople, D. P. Santry, G. A. Segal, *J. Chem. Phys.* **43**, S129 (1965); J. A. Pople, G. A. Segal, *J. Chem. Phys.* **43**, S136 (1965); **44**, 3289 (1966); see also: P. Birner, H. J. Koehler, C. Weiss, *Chem. Phys. Lett.* **27**, 347 (1974); H. J. Hofmann, P. Birner, *Chem. Phys. Lett.* **37**, 608 (1976).

[9] S. Diner, J. P. Malrieu, F. Jordan, M. Gilbert, *Theor. Chim. Acta* **15**, 100 (1969), and references therein.

[10] For a recent review see R. F. W. Bader, R. A. Gangi, *A Specialist Periodical Report, Theoretical Chemistry*, Vol. 2, p. 1, The Chemical Society (London), Burlington House, London 1975.

[11] (a) H. Eyring, M. Polanyi, *Z. Physik. Chem.* (Leipzig) **B12**, 279 (1931); for a general review of calculations see Ref. [1a]; (b) S. Sato, *Bull. Chem. Soc. Jap.* **28**, 450 (1955); *J. Chem. Phys.* **23**, 592, 2465 (1955); (c) R. N. Porter, M. Karplus, *J. Chem. Phys.* **44**, 1105 (1964); see also L. Pedersen, R. N. Porter, *J. Chem. Phys.* **47**, 4751 (1967); (d) L. M. Raff, L. Stivers, R. N. Porter, D. L. Thompson, L. B. Sims, *J. Chem. Phys.* **52**, 3449 (1970); (e) for a recent review see P. J. Kuntz, *Modern Theoretical Chemistry*, Vol. 2 (Dynamics of Molecular Collisions, Part B), W. H. Miller, Ed., Plenum Press, New York and London 1976, p. 53.

[12] (a) F. O. Ellison, *J. Am. Chem. Soc.* **85**, 3540 (1963); (b) J. C. Tully, *J. Chem. Phys.* **58**, 1396 (1973); (c) P. J. Kuntz, A. C. Roach, *J. Chem. Soc. Faraday Trans. II*, **68**, 259 (1972); P. J. Kuntz, *Chem. Phys. Lett.* **16**, 581 (1972).

[13] (a) F. T. Wall, R. N. Porter, *J. Chem. Phys.* **36**, 3256 (1962); **39**, 3112 (1963); (b) N. C. Blais, D. L. Bunker, *J. Chem. Phys.* **37**, 2713 (1962); **39**, 315 (1963); (c) D. L. Bunker, *Methods Comput. Phys.* **10**, 287 (1971).

[14] (a) K. Fukui, *J. Phys. Chem.* **74**, 4161 (1970); (b) K. Fukui, *Reactivity and Structure, Concepts in Organic Chemistry*, Vol. 2 (Theory of Orientation and Stereoselection), Springer-Verlag, Berlin 1975, p. 102; (c) K. Fukui, in *The World of Quantum Chemistry* (Proceedings of the First International Congress of Quantum Chemistry Held at Menton, France, July 4–10, 1973), R. Daudel, B. Pulman Eds., D. Reidel, Dordrecht 1974, p. 113; (d) K. Fukui, S. Kato, H. Fujimoto, *J. Am. Chem. Soc.* **97**, 1 (1975); (e) S. Kato, H. Kato, K. Fukui, *J. Am. Chem. Soc.* **99**, 684 (1977).

[15] (a) R. F. W. Bader, *Canad. J. Chem.* **40**, 1164 (1962); (b) R. B. Woodward, R. Hoffmann, *J. Am. Chem. Soc.* **87**, 395, 2046, 2511 (1965); see also R. B. Woodward, R. Hoffmann, *The Conservation of Orbital Symmetry*, Verlag Chemie Weiheim/Bergstr., Germany 1970; (c) J. N. Murrell, K. J. Laidler, *Trans. Faraday Soc.* **64**, 371 (1968); (d) J. N. Murrell, G. L. Pratt, *Trans. Faraday Soc.* **66**, 1680 (1970); (e) R. G. Pearson, *Acc. Chem. Res.* **4**, 152 (1971); (f) K. Fukui, *Acc. Chem. Res.* **4**, 57 (1971); (g) J. W. McIver, R. E. Stanton, *J. Am. Chem. Soc.* **94**, 8618 (1972); J. W. McIver, *Acc. Chem. Res.* **7**, 72 (1973); R. E. Stanton, J. W. McIver, *J. Am. Chem. Soc.* **97**, 3632 (1975); (h) W. A. Goddard, *J. Am. Chem. Soc.* **94**, 793 (1972).

[16] P. Empedocles, *Int. J. Quant. Chem.* **3**, 47 (1969).

[17] (a) J. W. McIver, A. Komornicki, *J. Am. Chem. Soc.* **94**, 2625 (1971); (b) A. Komornicki, J. W. McIver, *J. Am. Chem. Soc.* **95**, 4512 (1973).

[18] M. J. S. Dewar, S. Kirschner, *J. Am. Chem. Soc.* **93**, 4290, 4291, 4292 (1971).

[19] (a) J. Pančíř, *Collect. Czech. Chem. Commun.* **40**, 1112 (1975); (b) Z. Slanina, *Collect. Czech. Chem. Commun.* **39**, 3187 (1974).
[20] T. A. Halgren, I. M. Peppenberg, W. N. Lipscomb, *J. Am. Chem. Soc.* **97**, 1248 (1975).
[21] O. Ermer, *J. Am. Chem. Soc.* **98**, 3964 (1976).
[22] P. W. Dillon, G. R. Underwood, *J. Am. Chem. Soc.* **99**, 2435 (1977).
[23] K. Morokuma, K. Ishida, A. Komornicki, *Direct Determination of Saddle Points and Reaction Coordinates on ab initio Multidimensional Potential Energy Surfaces*, contributed paper, Second International Congress of Quantum Chemistry, New Orleans, April 1976.
[24] For a recent general review see M. C. Flanigan, A. Komornicki, J. W. McIver, *Modern Theoretical Chemistry*, Vol. 8 (Semiempirical Methods of Electronic Structure Calculation, Part B: Applications), G. A. Segal, Ed., Plenum Press, New York and London 1977, p. 14.
[25] (a) D. M. Silver, *J. Chem. Phys.* **57**, 586 (1972); (b) E. A. McCullough, D. M. Silver, *J. Chem. Phys.* **62**, 4050 (1975); (c) P. Mathias, W. A. Sanders, *J. Chem. Phys.* **64**, 3893 (1976).
[26] (a) R. Marcus, *J. Chem. Phys.* **45**, 4493 (1966); **49**, 2610 (1968); (b) J. C. Light, *Adv. Chem. Phys.* **19**, 1 (1971).
[27] (a) H. S. Johnston, C. Parr, *J. Am. Chem. Soc.* **85**, 2544 (1963); see also H. S. Johnston, *Gas Phase Reaction Rate Theory*, Ronald Press, New York 1966; (b) D. G. Truhlar, *J. Am. Chem. Soc.* **94**, 7584 (1972); (c) N. Agmon, *Chem. Phys. Lett.* **45**, 343 (1977).
[28] L. Pauling, *J. Am. Chem. Soc.* **69**, 542 (1947).
[29] I. Shavitt, R. M. Stevens, F. L. Minn, M. Karplus, *J. Chem. Phys.* **48**, 2700 (1968), normal-coordinate least-squares fit to "Surface II".
[30] J. T. Muckermann, *J. Chem. Phys.* **54**, 1155 (1970).
[31] M. J. S. Dewar, *Angew. Chem. Intern. Ed. Engl.* **10**, 761 (1971).
[32] P.-O. Löwdin, *Adv. Quant. Chem.* **2**, 213 (1965).
[33] (a) R. F. Nalewajski, A. Gołębiewski, *Acta Phys. Pol.* **A49**, 683 (1976); (b) R. F. Nalewajski, *J. Mol. Struct.* in press; (c) R. F. Nalewajski, *Z. Naturforsch.* **32a**, 276 (1977).
[34] P. Pulay, *Mol. Phys.* **17**, 197 (1969).
[35] P. W. Payne, *J. Chem. Phys.* **65**, 1920 (1976).
[36] Y. Jean, X. Chapuisat, *J. Am. Chem. Soc.* **96**, 6911 (1974).
[37] R. N. Porter, R. M. Stevens, M. Karplus, *J. Chem. Phys.* **49**, 5163 (1968).
[38] M. J. D. Powell, *Comput. J.* **7**, 303 (1965).